Chapter 4

Vertical Field Anomaly Map

4.1 Comparison of observed and *initial model* vertical field anomaly map

The global Vertically Integrated Susceptibility (VIS) model derived in chapter 2 is used to compute the vertical field anomaly map or the z-component map following the modelling procedure described in chapter 3. The spherical harmonic degrees 1-15 of the vertical field anomaly map are set to zero because this long wavelength crustal field is masked by the main field and is not observable. Hence, only spherical harmonic degrees 16-80 of the model field are computed and are compared with the corresponding degrees 16-80 of the observed crustal field. The results are discussed for all the major anomalies observed over the continents and oceanic regions in the following subsections.

In Chapter 2, when the two global seismic crustal models were introduced it was mentioned that only one of them would be selected for our modelling work. To start with, both 3SMAC and CRUST2.1 crustal model were considered for deriving VIS model. The vertical field anomaly map produced using the VIS models derived using both the crustal models did not vary much over the oceans but over the continents there was some mismatch. Significant disagreement of the magnetic anomaly patterns was seen over Africa, Greenland, northern Siberia, eastern Tibetan plateau, South America and most of eastern region of North American craton. Except over the North American craton, where the magnetic anomaly map produced using the CRUST2.1 matched more closely with the observed anomaly map, for rest of the regions mentioned above, 3SMAC model produced a better fit with the observed. Thus, CRUST2.1 model is used for modelling the North American craton and 3SMAC model for the rest of the world including the oceans. There are obvious gaps in the seismic models of both 3SMAC and CRUST2.1 in the African region, Greenland and South America. So, the new seismic results for Greenland (Dahl-Jensen et.al, 2003) and for Guyana shield, South America (Schmitz et al., 2002) is used in the derivation of initial VIS model, instead of 3SMAC or CRUST2.1 model for these regions. For Africa, however, 3SMAC seismic model is retained. This is because 3SAMC model is derived using both seismological and nonseismological constraints such as chemical composition, heat flow, hotspot distribution, from which estimates of seismic velocities and the density in each layer is made. While the CRUST2.1 model is only a minor improvement over its predecessor CRUST5.1, and includes only the compilation of seismic data across the globe and the gaps were filled by applying a statistical average for various geological settings such as Precambrian shields, extended

continental crust and passive margins. Thus, the better constrain of 3SMAC model using nonseismic data and due to a better fit of the predicted vertical field anomaly map with the observed map, 3SMAC seismic model is used for modelling most part of the world, except North America, Greenland and Guyana shield of South America, where seismic models as stated above has been used.

The CHAMP observed vertical field anomaly map is shown in Figure (4.1) and the corresponding global vertical field anomaly map predicted using the initial VIS model is shown in Figure (4.2). The two maps are compared visually. On comparison it is apparent that there are anomalies over the regions where the *initial model* and observed maps match well while there are anomaly patterns that do not match. Over some regions the predicted anomalies display higher amplitude than the observations. The effect of continent-ocean boundary is also not apparent in the computed map and needs further discussion. There are East-West trending anomaly patterns over the oceanic region in the observed map, which are absent in the predicted map, especially over the Pacific Ocean. The anomaly patterns related to oceanic rises and plateaus agree well, especially those located south east of African continent, while only partially in the regions south west of it. This suggests that the seismic thickness of most of these plateaus needs to be redefined. A comparison of observed and *initial model* maps is now being described for all the continents and oceanic regions.

4.2 Examples of predicted anomalies in agreement and in disagreement with observed anomaly map

4.2.1 Cathaysian craton

The Cathaysian craton has been studied by others using the crustal field observed by Magsat data. Total field anomaly maps were derived and the sources of anomalies were associated with the corresponding geological units (Achache et al., 1987; Arkani-Hamed et al., 1988). Similar results have been reported for the Tibetan plateau for vertical field anomaly maps by Arkani-Hamed et al. (1988), Rajaram and Langel (1992), Hamoudi et al. (1995) and very recently by Alsdorf and Nelson (1999). The Indian craton has also been studied extensively using the vertical field (Mishra, 1984; Agarwal et al., 1986; Rajaram and Langel, 1992) and total field anomaly maps (Negi et al., 1986; Singh and Rajaram, 1990) using Magsat data.

The Cathaysian craton exhibits diverse geological units including the Himalayan fold belt and is modeled here using the susceptibility distribution for each of these units (Appendix III) following the modelling procedure described in Chapter 2. The tectonic map for the Cathaysian craton is shown in Figure (2.1) and for the Indian craton in Figure (2.8). The *initial model* vertical field anomaly map is computed at the satellite altitude of 400 km and is compared with the corresponding observed vertical field anomaly map.

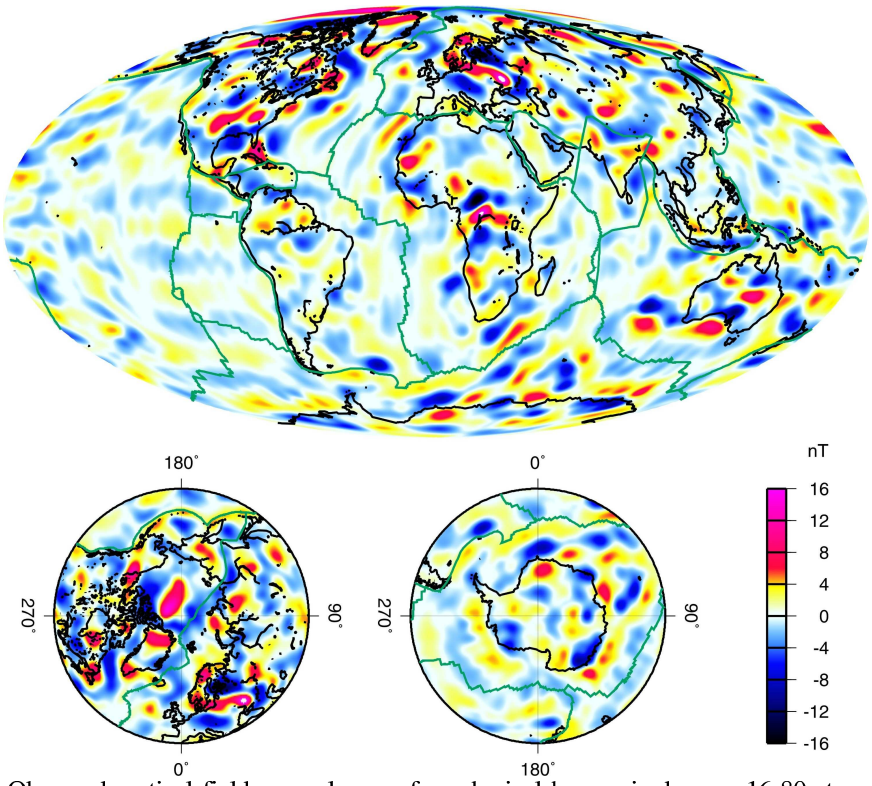

Fig. 4.1. Observed vertical field anomaly map for spherical harmonic degrees 16-80 at an altitude of 400 km.

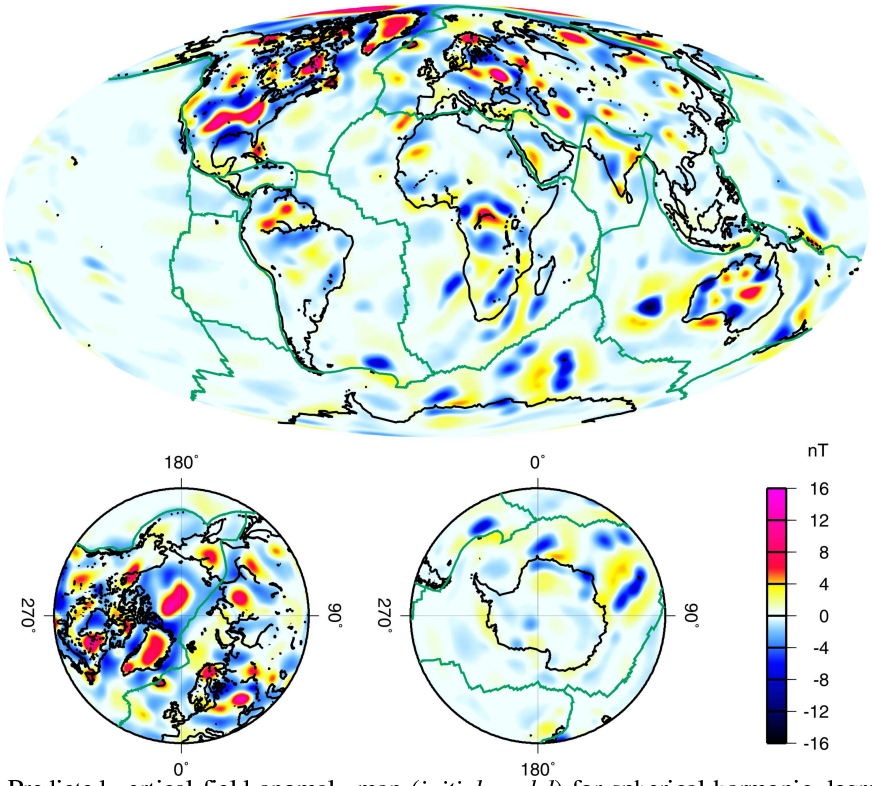

Fig. 4.2. Predicted vertical field anomaly map (*initial model*) for spherical harmonic degrees 16-80 at an altitude of 400 km.

The observed vertical field anomaly map for the Cathaysian craton is shown in Figure (4.3a). A large positive anomaly is observed over Tarim basin, (1), that not only is observed over the Archean rocks exposed at the core of the basin but also extends over the surrounding Proterozoic rocks overlain by Mesozoic-Cenozoic cover. Further towards east, over the Yangtze craton, lies a positive anomaly of moderate amplitude attributed to the Sichuan massif, (2). A large positive anomaly can also be seen over the largely buried Songliao microcontinent, (3), north of the Korean peninsula. The most interesting of all the anomalies is the strong negative observed over the entire stretch of the Himalayan fold belt and the Tibetan plateau, (4), suggesting a non-magnetic character of the lower crust in the region. Further, located southeast of the Caspian sea is a circular shaped anomaly overlying the Turkmenistan shield, (5).

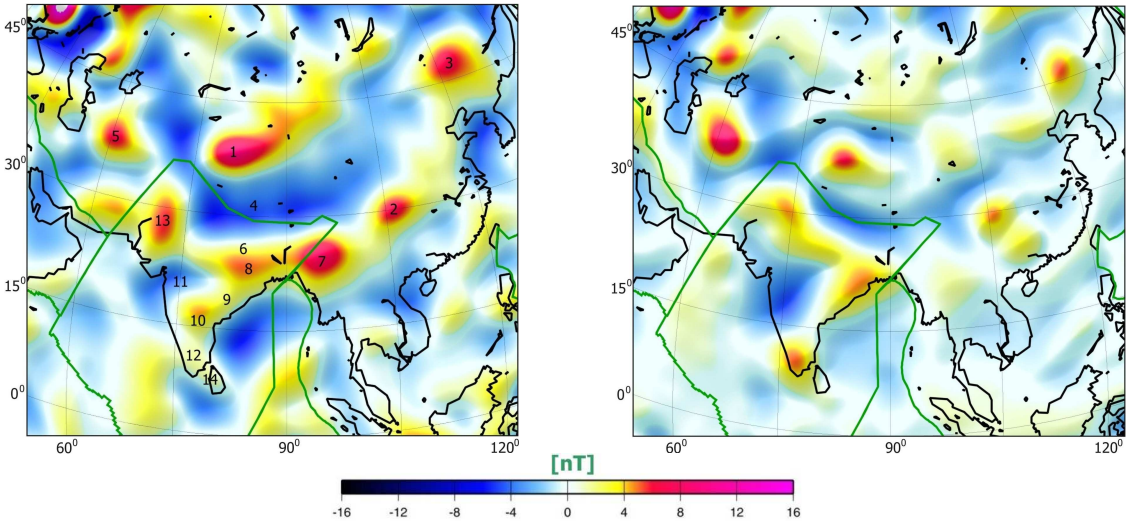

Fig. 4.3a. Observed vertical field anomaly map for spherical harmonic degrees 16-80 at an altitude of 400 km for the Cathaysian craton and Indian subcontinent.

Fig. 4.3b. *Initial model* vertical field anomaly map for spherical harmonic degrees 16-80 at an altitude of 400 km for the Cathaysian craton and Indian subcontinent.

South of the Cathaysian craton lies the Indian subcontinent. A positive anomaly of moderate intensity is observed all along the Indo-Gangetic basin, (6), south of Himalayan fold belt. These anomaly patterns terminate at the North Eastern border of India, in Myanmar, (7), where a large circular anomaly is seen. A positive anomaly is also observed over the Singhbhum craton, (8), east of Bangladesh. Further south, within the subcontinent, a stretched out positive anomaly of moderate intensity follows the eastern border of Peninsular India, (9) which terminates over the Eastern Dharwar craton, (10). In the west, a negative anomaly over the Narmada-Son basin, (11), is observed. Southern India peninsular gneiss (12), exhibits a weak negative anomaly at satellite altitude. An anomaly aligned north-south is also observed extending from the western border of Gujarat, India to central Pakistan, (13). A very weak positive anomaly is also seen over the Proterozoic provinces of SriLanka, (14).

The *initial model* vertical component anomaly map for Cathaysian-Indian region is shown in Figure (4.3b). The large anomaly over the Tarim basin agrees well only over the central region where the Archean rocks are exposed while the rest of the basin,

assumed as essentially non-magnetic, does not agree with the observations. It is important to note that Archean rocks, exposed only at the core of the basin, fail to explain an anomaly of such large amplitude and shape. Rather, it appears that the basement Archean rocks extend further below the Proterozoic province of the Tarim microcontinent and the observed anomaly shape indicates the bulk effect of such a mafic basement structure. This needs further investigation to find the source of the missing anomaly and is discussed in Chapter 5. A positive anomaly seen over largely buried Songliao microcontinent, is reproduced only partially in the *initial model*. The westward extension of the predicted anomaly is completely missing. This suggests the presence of a still larger buried microcontinent. A moderate positive anomaly predicted for the Sichuan massif of the Yangtze craton relates well with the observed one; however, a part of the amplitude of the anomaly is yet unaccounted for. Over the Turkmenistan shield, located southeast of the Caspian sea, the predicted and observed anomaly maps are in complete agreement.

The predicted strong negative anomaly region over the Himalayan fold belt and the Tibetan plateau agrees well with the extension of the measured anomaly. However, a part of the anomaly is not reproduced. It is to be noted that the susceptibility value for the rock types exposed in the Himalayan fold belts (Appendix III) is already very low yet the observed anomaly warrants still lower susceptibility value for the region. Another possible reason for such low magnetisation could be a high heat flow in the region and the lower crust could be almost non-magnetic. As the heat flow models have not been a part of our modelling, the possibility of a shallow Curie-temperature isotherm is not investigated here. Alsdorf and Nelson (1999) investigated the magnetic anomaly map derived using Magsat data and concluded that high heat flow in the Tibetan plateau could be a cause for the intense low anomaly pattern.

On the Indian subcontinent, the *initial model* magnetic anomaly map computed at satellite altitude fails to reproduce most of the large-scale observed anomalies, except over the regions of Indo-Gangetic plains lying south of the Himalayan fold belts, and some shield regions of India. The anomalies over the Myanmar region, east of the Indian shield, and in Pakistan to the west, are not reproduced in the predicted anomaly map. Lack of information on geological features overlain by Phanerozoic cover in south-central Pakistan is partially responsible. In the east, the complex interaction of the Indian plate with the Cathaysian plate has deformed them, and an active subduction in the region (Satyabala, 1998) can be a possible source for the observed anomaly pattern over Myanmar. This subducting plate has not been modeled in the present modelling method. The anomalies over eastern peninsular India agree well with the observations, though the circular feature over the Eastern Dharwar region in the observed map is completely absent in the predicted map. The negative anomaly over the Narmada-Son basin appears to extend in the south direction over the Deccan plateau. It is apparent from the results for the entire subcontinent that the nature of its lower crust and also its interaction with Cathaysian plate need to be understood properly.

4.2.2 Siberian craton

Satellite derived magnetic anomaly maps have rarely been used to study this craton and the work is restricted to map the Kursk anomaly, Russia. Taylor and Frawley (1987) derived scalar and vector maps to study the Kursk anomaly while Ravat et al. (1993) used only scalar maps to model the anomalies.

The observed vertical field magnetic anomaly map for the Siberian craton, shown in Figure (4.4a), shows the major anomalies associated with the shield region. In the north, a positive anomaly is associated with the Anabar shield, (1), however the anomaly extends further northwest over the Phanerozoic Khatanga trough, (2). An anomaly of moderate intensity is associated with the Vilyuy syneclise, (3), located southeast of the Anabar shield. Further southeast of this syneclise lies a positive anomaly over the Aldan shield, (4), and partly over the Aldan anteclise, (5). At the southern tip of the Siberian craton lies an anomaly trending parallel to the eastern flank of Baikal lake, (6). This anomaly overlies the southern half region of Baikal fold belt. A strong negative anomaly is observed north of Aldan shield, which follow the meandering east-northeast boundary of Siberian craton and is associated with the basin region of the Verkhoyansk fold belt, (7), in the north and Okhotsk-Chauna fold belt, (8), in the south. Further east of Verkhoyansk fold belt a positive anomaly can be observed that lies all along the eastern flank of Cherskiy suture zone, terminating north of Kamchatka peninsula. This anomaly is attributed to the partly buried Kolyma block, (9), that got accreted along with Omolon massif, to the northeast Siberia (Fujita, 1978).

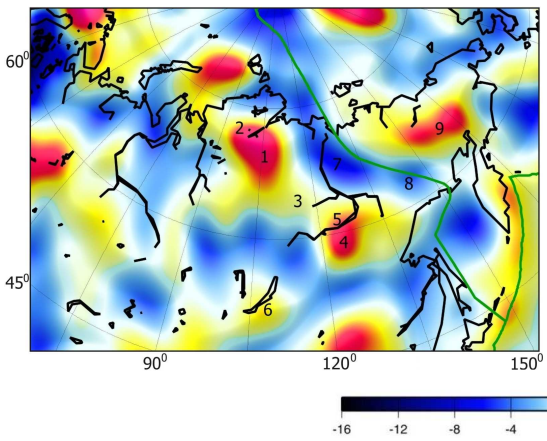

Fig. 4.4a. Observed vertical field anomaly map for spherical harmonic degrees 16-80 at an altitude of 400 km for the Siberian craton.

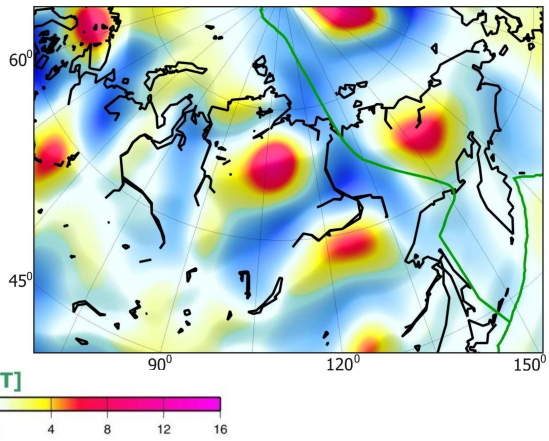

Fig 4.4b. *Initial model* vertical field anomaly map for spherical harmonic degrees 16-80 at an altitude of 400 km for the Siberian craton.

The *initial model* map for the Siberian craton (Fig. 4.4b) is calculated using the susceptibility distribution for geological units as mentioned in Appendix (IV). The tectonic map for the Siberian craton is shown in Figure (2.2). Over the Anabar shield in the north, a large positive anomaly can be compared with that of the anomaly of the observed map, however, the northwestward extension of the observed anomaly over the Khatanga trough is completely missing from the predicted map. This result points to our limited knowledge of the subsurface extension of Anabar shield, especially in the

northwest direction. An anomaly over the Aldan shield in the southwest Siberian craton agrees well with the observed anomaly, although a part of the anomaly is yet unaccounted for. A negative anomaly observed over the Verkhoyansk fold belt, extending all along to the Okhotsk sea, is in good agreement with the observations. A positive anomaly appears over the northern and southern region of Baikal fold belt. This differs from the observed map where the anomaly is observed only at the center of the fold belt.

Kolyma block is modelled based on the study of Sweeney (1981), and *initial model* vertical field anomaly map is computed over the region. Considering the subsurface extension of the block as envisaged by Sweeney (1981), the predicted anomaly does not match the observed anomaly pattern, although the amplitude agrees very well. This anomaly is reinvestigated in detail in Chapter 5 to redefine the boundary of this block.

4.2.3 East European craton

The East European craton has been most extensively studied using the satellite data. Since it hosts some of the largest magnetic anomalies at satellite altitude, it has drawn lots of attention to interpret them. Maps derived using only Magsat data include the work of Arkani-Hamed and Strangway (1986b), DeSantis et al. (1989), Cain et al. (1989b), Nolte and Hahn (1992), Ravat et al. (1993) and Taylor and Ravat (1995).

The East European craton includes diverse geological features. The CHAMP observed magnetic anomaly map shown in Figure (4.5a) reveals the anomaly features corresponding to some of these geological bodies. In the north, within the Baltic shield, an intense positive anomaly is observed over the Kiruna mines, (1), in north Sweden. A strong negative anomaly is observed south of it over the Svecofennian domain, (2), and the southern Karelian province, (3), in the north and over Moscow syneclise, (4), in the centre of the East European craton. Further south, east of the Ukranian shield, is situated one of the largest positive anomalies on the global magnetic anomaly map. This anomaly, called 'Kursk Anomaly' is associated with the iron formations of Voronezh anteclise, (5), Russia. An anomaly corresponding to the Ukranian shield, (6), is almost non-existent at satellite altitude. A positive anomaly follows the western border of the craton marked by the TTZ (Tornquist-Teisseyre Zone), (7), extends into the Baltic sea, (8), and terminates in the southwest Scandinavian, (9), region. Apart from the Belorussian uplift, (10), located north of the Ukranian shield, there is no other geological affinity to the anomaly pattern observed. Another interesting anomaly feature is observed over the southern Ural mountains, (11), with its westward extension further inside the craton, partly overlying the Volga-Urals anteclise and Tatarian swells, (12).

The vertical field magnetic anomaly map computed at a satellite altitude of 400 km using the susceptibility distribution described for various geological units in Appendix (V), is shown in Figure (4.5b). The tectonic map for the East European craton is shown in Figure (2.3). A positive anomaly observed over the Kiruna mines is associated with iron formations in the region and is reproduced well in the *initial model* map. A negative anomaly observed over the Moscow syneclise and regions of the southern Baltic shield is

due to the removal of long-wavelength anomaly associated with a basement of craton. This may partly be due to thick Phanerozoic cover over the Moscow syneclise, however, some part of the anomaly is yet unaccounted for. The anomaly computed over the Voronezh anteclise is in agreement with the Kursk magnetic anomaly observed over this region. This anomaly is associated with early Proterozoic iron formations in the region, which extends for more than 1000 km (Goodwin, 1991). The extended anomaly pattern computed along the TTZ shows a similar trend as has been observed. However, the anomaly is not reproduced in the north, especially over the Baltic sea and in the southwest Scandinavian domain. The modelling results indicate that the anomaly along the TTZ is produced due to the bulk susceptibility contrast of the thick crust in the west and thinner on the east and is not due to any geological body of high susceptibility lying along the zone except for the Belorussian anteclise. The anomalies over the central Urals and Volga-Urals anteclise also agree well with the observed map.

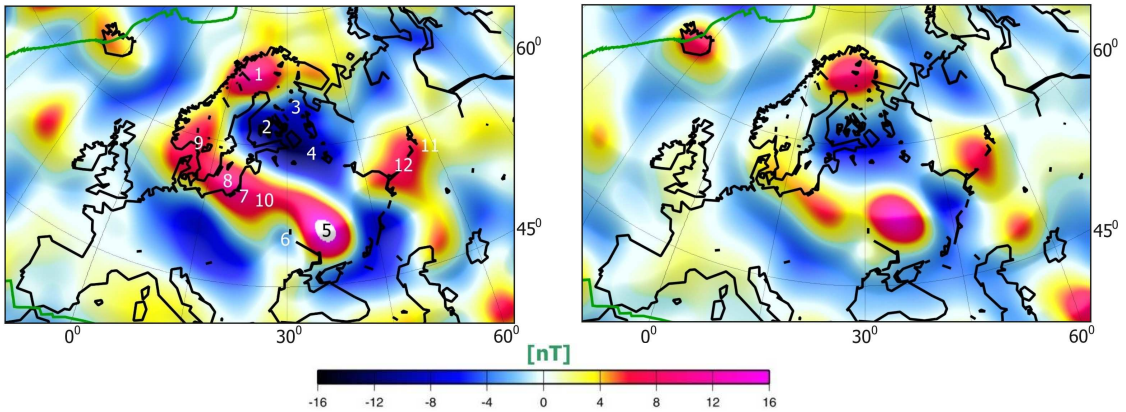

Fig. 4.5a. Observed vertical field anomaly map for spherical harmonic degrees 16-80 at an altitude of 400 km for the European craton.

Fig. 4.5b. *Initial model* vertical field anomaly map for spherical harmonic degrees 16-80 at an altitude of 400 km for the European craton.

An unresolved question about the East European craton basement is its extent. Deep drilling results for the basement of craton provide 23 known Archean units filled in by early Proterozoic rocks (Goodwin, 1991). However, the extension of these units is largely open to speculation. In the derivation of initial VIS model the basement is assumed below the craton at all the regions except south of Voronezh anteclise. There is consistent variation of sediment thickness from north to south of the craton. It is 0-2 km in the north and 4-6 km over the Moscow syneclise in the center and more than 23 km thick (Khain, 1985) over the north Caspian sea syneclise in the south. In spite of such a craton structure a strong positive anomaly was expected over the center of craton. On the contrary a negative anomaly is noticed over the Moscow syneclise and southern Baltic shield and a strong positive anomaly along the TTZ. The *initial model* matches well with the observed pattern over the center of craton. This means the basement behave as a single large unit and long wavelength associated with the craton is removed with the removal of spherical harmonic degrees 1-15. This may produce the negative over the center of craton and positive over the western region along TTZ followed by a negative anomaly over the west of craton.

4.2.4 North American craton

The North American craton consists of a wide range of geologic bodies and has been studied extensively by both surveys of surface geology and geophysical investigations of the lithosphere. The satellite anomaly maps have been derived to fill the gaps in these studies, especially in the geophysical surveys. This is helpful for developing an hypothesis for the origin of magnetic signatures in less well-known or exposed regions of the Earth. Some of the earlier studies in this regard have been carried out for the United States by Mayhew (1982a) and Langel (1990) using Magsat and POGO satellite data. For the mid continent region, Carmichael and Black (1986) and for lower crustal thickness variation by Schnetzler (1985). Whaler and Langel (1996) prepared a magnetisation map of the United States from Magsat data while and Purucker et al. (2002) used both Magsat and Ørsted data. The northern part of the large continent, the Canadian shield region, has also been studied by Langel et al. (1980) and Arkani-Hamed et al. (1984). The observed vertical field magnetic anomaly map of the North American craton is shown in Figure (4.6a) and the *initial model* magnetic anomaly map in Figure (4.6b).

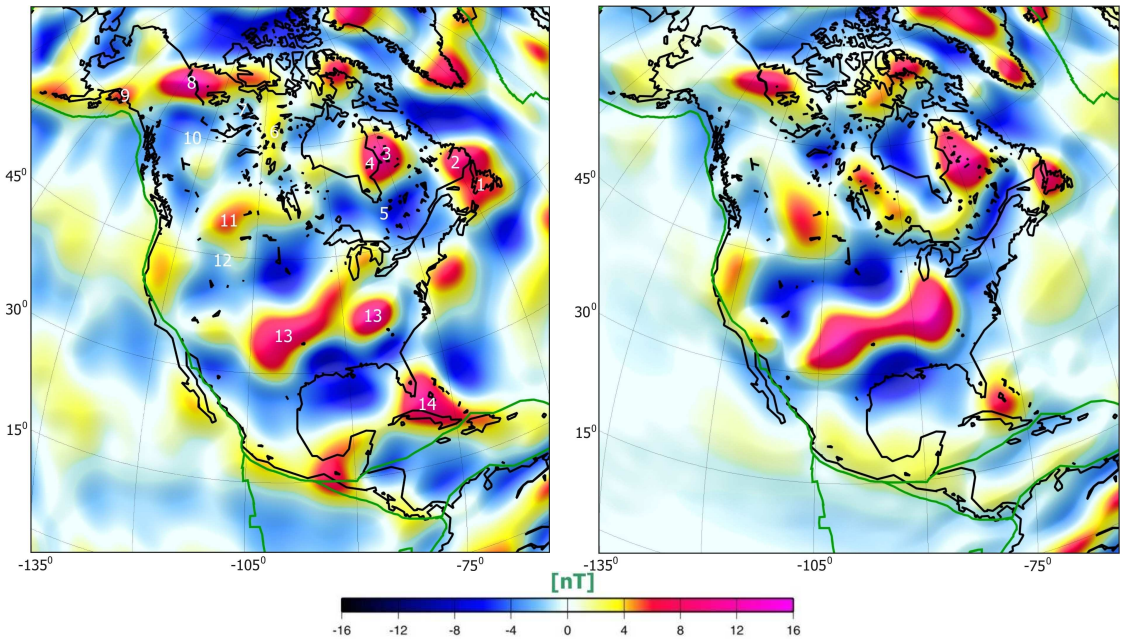

Fig. 4.6a. Observed vertical field anomaly map for spherical harmonic degrees 16-80 at an altitude of 400 km for the North American craton.

Fig. 4.6b. *Initial model* vertical field anomaly map for spherical harmonic degrees 16-80 at an altitude of 400 km for the North American craton.

The observed anomaly map shows scattered anomaly patterns all over the craton, mostly lying over the Precambrian units. In the northeastern region, a flattened bell- shaped positive anomaly is observed over Newfoundland, (1), that extends further north over the eastern region of Grenville province, (2). Northwest to this anomaly, within the Superior province, a large oval-shaped anomaly lies over the Ungava craton, (3), and part of Belcher iron formations, (4), in Hudson Bay. Regions south and southeast of Hudson bay, (5), are characterised by a negative anomaly of moderate intensity. The regions west of Hudson Bay, over the Churchill province, (6), show a weak positive anomaly which

stretches in a north-south direction. Interestingly, the Archean Slave province, (7), appears almost non-magnetic at satellite altitude. Located in the northwest region of the craton, there is a large elongated positive anomaly, (8), extending from Slave craton to the Yukon province of Canada. This large stretch of anomalies lies over the Wopmay orogenic units, primarily exposed only in the northwestern region of the Slave craton and partially buried further west of it. Small positive anomaly features, (9), extend to the Bering Sea along the Aleutian arc and are attributed, within the continents, to the exotic terrains accreted to the Cordilleran units of the North American craton (Sweeney, 1981). A weak anomaly pattern southeast of Wopmay orogen is observed over the Mackenzie-Wernecke mountains, (10), of Proterozoic age. An intense positive anomaly, (11), also appears north of Wyoming province, (12), whose source regions are yet to be determined, because of the thick Phanerozoic cover that masks the underlying structure. Further to the south of this large craton, over southwest USA, (13), lies one of the largest stretches of satellite-altitude anomalies on Earth. These anomalies lie over the mid-Proterozoic provinces, dominated by anorogenic granite intrusions in the crust. Lastly, a positive anomaly, (14), can be observed extending from the banks of Florida to the Bahamas Island. The origin of these anomalies is yet unresolved, as it is generally attributed to the underlying oceanic crust, and few believe that it is due to continental crust.

Global seismic crustal model CRUST2.1, a higher resolution model of its predecessor CRUST5.1 (Mooney et al., 1998), is known to be much more accurate in the North American craton, especially in the western region of the craton, than estimated by 3SMAC seismic model. Thus, CRUST2.1 model is preferred over the 3SMAC model for the VIS computation for North American craton. Using the susceptibility distribution for various units of the North American craton as shown in Appendix (VI), *initial model* vertical field anomaly map is computed at an altitude of 400 km. The tectonic map for the North American craton is shown in Figure (2.5). A comparison is done with the observed anomaly map for the corresponding regions. The region of Newfoundland is known for ophiolite accretion during the Taconic orogeny, mid Ordovician (Colman-Sadd, 1980). Bay of Island and its surrounding region occupy more than a 100 km stretch of ophiolites (Colmann-Sadd, 1980). The anomalies predicted over this region show a positive only over the Newfoundland region in agreement with the observations. The part of anomaly over the Grenville province northwest of Newfoundland, however, is not reproduced.

The predicted anomaly over the Ungava province of the Archean Superior province and its extension over the Belcher iron formations in the Hudson Bay show a good correspondence with the observed map. An extended positive anomaly pattern of moderate intensity over the southwest region of Superior province is in disagreement with observations, which show a corresponding negative anomaly. A similar positive anomaly of moderate intensity, stretching in the north-south direction, located west of Hudson Bay over the Churchill province, is not reproduced in the *initial model* magnetic anomaly map. An intense positive anomaly predicted over the Wopmay orogen, overlain by Phanerozoic cover in the Yukon state, shows a good resemblance with the observed magnetic map. Further south in Mackenzie state, the anomaly over the Mackenzie mountains also shows a good correlation with the observations. However, the east-west trending positive anomaly south of it and north of Wyoming uplift is reproduced only

partially. The moderate positive observed over the western coast of the USA, attributed to the accreted Arc terrain during Permian-Triassic era (Dickinson, 1981), matches the observed anomaly pattern over the same region.

In the southeast USA, the large stretch of anomaly over the Kentucky-Tennessee region characterized by the mid-Proterozoic anorogenic granite province is reproduced reasonably well; however, the predicted anomaly pattern does not follow the boundary of the observed anomaly. Apparently, this region needs to be investigated in detail to redefine the boundary of this mid-Proterozoic province, as it is largely buried under Phanerozoic cover. The results of investigation are shown in chapter (5).

The positive anomaly over the region of the Bahamas Islands is reproduced well. However, its extension to the bank of Florida is not evident in the *initial model* anomaly map. This indicates a more extended oceanic crust beyond the political boundary of Florida and the Bahamas. The modelling results indicate that this anomaly is due to oceanic crust, as the crust of continental origin is unable to reproduce such intense anomaly patterns.

4.2.5 South American craton

Shield regions dominate the northern part of the South American craton and the Precambrian Sao Francisco and Ribeira belts occupy the central-eastern region of the craton. This craton has generally been a target of study to find the continuation of rock types from its eastern region to the western region of mid-Africa prior to the Gondwana break-up. Some of the work in this respect and in general to map the sources for magnetic anomalies over South America has been carried out by Hinze et al. (1982), Ridgway and Hinze (1986), von Frese et al. (1989) and Ravat et al. (1991). They prepared scalar anomaly maps using Magsat satellite data.

The entire continent appears non-magnetic except for the shield regions as shown in the Figure (4.7a). Over the Guyana Shield in the north, the observed vertical field anomaly map shows a moderate positive anomaly both in the northern, (1), and southern flanks, (2). A negative anomaly, (3), is observed over the northern part of the Brazilian shield. This anomaly extends further northwest, (4), over the basin of Amazon river. At the mouth of the Amazon river, (5), a positive anomaly over the sedimentary basin is observed that overlie partly the San Ignacio mobile belt. Further southeast, an anomaly of moderate intensity lies over the Sao Francisco belt, (6), and Ribeira belt, (7), that extends partly into the South Atlantic Ocean.

The vertical field anomaly map for the South American continent is computed using the susceptibility distribution given in Appendix (VII) and is shown in Figure (4.7b). The tectonic map for the South American craton is shown in Figure (2.6). For Guyana shield regions, in South America, the new seismic crustal model of Schmitz et al. (2002) was included in place of 3SMAC model.

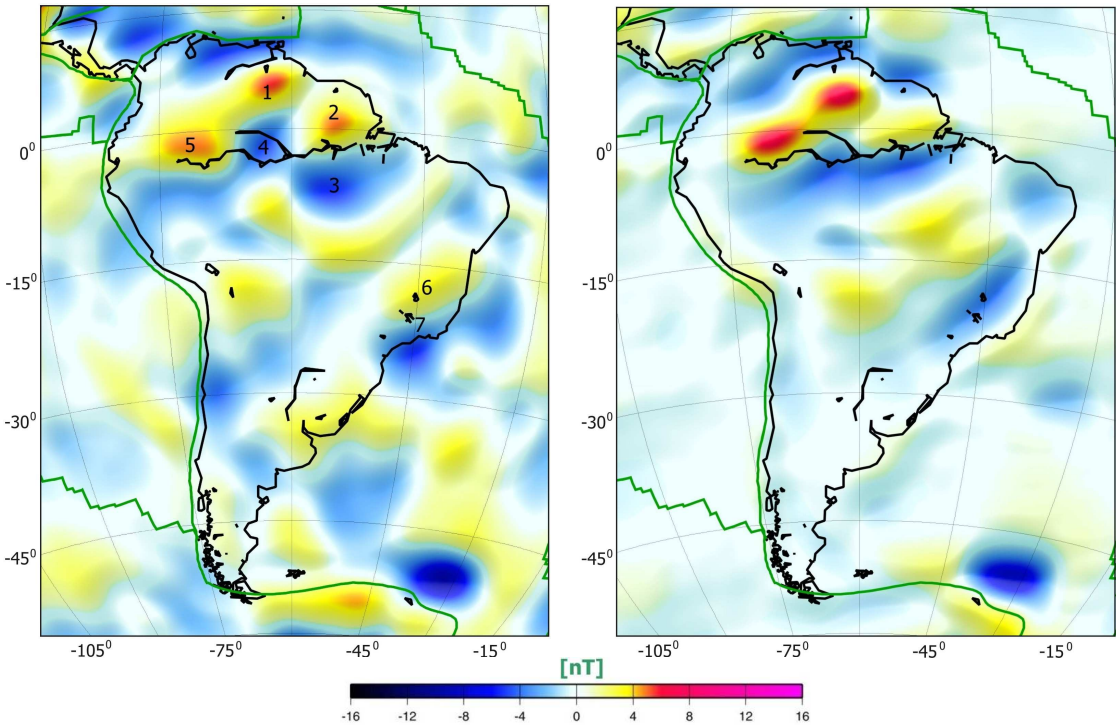

Fig. 4.7a. Observed vertical field anomaly map for spherical harmonic degrees 16-80 at an altitude of 400 km for the South American craton.

Fig. 4.7b. *Initial model* vertical field anomaly map for spherical harmonic degrees 16-80 at an altitude of 400 km for the South American craton.

A comparison of the *initial model* anomaly map with the observed anomaly map (Fig. 4.7a) suggests a good agreement of the anomaly pattern. The positive anomalies predicted over the shield regions is in agreement with the observations, suggesting their sources to lie within the Precambrian units of the shield regions, though they are stronger in amplitude than the observed anomalies. The anomaly observed over the north Guyana shield is located further north over the southern bank of Orinoco river, suggesting the greenstone belts units of Guyana shield, producing these anomalies, extend further north below the Phanerozoic cover. A positive anomaly over the sedimentary basin of the Amazon river, overlying the San Ignacio mobile belt, is also reproduced reasonably well though the predicted anomaly appears still larger and stronger. A single hump-shaped negative anomaly observed at the center of the Amazon river however, is not exactly reproduced in the predicted map. The negative anomaly over the north Brazilian shield is also not reproduced. Further southeast, the positive anomaly observed over the San Francisco craton and Ribeira belt appears shifted north in the *initial model* map. The extension of the cratonic region into the ocean is not modelled in the present work due to lack of such data. However, based on the observed anomaly pattern over the oceanic region, a possible eastward extension of San Francisco belt in the Continental arc region cannot be ruled out.

The southern region of the South American craton is covered by Phanerozoic including the Andes. As the Phanerozoic cover is associated with a constant susceptibility value, the difference in VIS values can only arise due to variation in crustal thicknesses. The

predicted anomaly pattern from the *initial model* suggests no interesting anomalies over the southern South American craton, which is in disagreement with the observations. The observed anomaly map does show some magnetic anomaly features over the central Andes. This result indicates that variation of magnetic properties in the younger crust may be important in modelling crustal anomalies.

4.2.6 African craton

Not much is known of this large continent due to the scarcity of extensive ground geophysical surveys, especially in the interior of the craton. However, using satellite data there has been some effort to extract more information about the nature of the crust underlying the cratons and mobile belts. One of the most enigmatic magnetic anomalies lies in Central Africa, at Bangui. The source of the anomaly is considered to be geological by Regan and Marsh (1982) while Girdler et al. (1992) modeled the anomaly using an iron meteorite. The West African craton received similar attention by Ravat (1989) and Toft et al. (1992).

Using the geological and tectonic information of Africa (Goodwin, 1991) and their average susceptibilities as listed in Appendix VIII, the vertical field anomaly map is computed (Fig. 4.8a) and compared with the corresponding observed magnetic anomaly map (Fig. 4.8b). The tectonic map for the African craton is shown in Figure (2.7).

Over the West African Craton, the observed vertical field anomaly map shows a band of negative amplitude that extends over the Man shield, (1), and is strongest over the central region of Taudeni basin, (2). A negative anomaly is also observed over the Tindouf basin, (3), north of the Reguibat shield. A strong positive anomaly is observed over the Amsaga belt, (4), of the Reguibat shield, that partly overlies the northwestern region of Taudeni basin. A positive anomaly is also observed over the Archean Liberian shield, (5). This anomaly extends further southwards into the South Atlantic ocean. The entire Hoggar shield, (6), appears to be very weakly magnetic. Over the Benin-Nigeria shield in the southeast of West African craton, a positive anomaly is seen over Nigeria shield, (7), while the Benin shield, (8), appears non-magnetic. The *initial model* anomaly map does reproduce the negative anomaly over the Taudeni basin flanked by positive anomaly on either side, in agreement with satellite observations, but most of the amplitude is yet unaccounted for. The entire Hoggar shield appears non-magnetic, which agree partially with the observed anomaly map. Over the Benin-Nigeria shield a disagreement in the anomaly patterns between the predicted and observed map is evident over the Nigeria shield and agreement over the Benin shield.

In northeast Africa, the observed map shows no interesting anomaly features except over the Nubian-Arabian shield. The mid-Proterozoic Nubian shield, (9), is almost non-magnetic whereas the Arabian shield, (10), generates a positive. The computed map agrees well with the observed map, although the positive observed over the Arabian shield appears further south in the Arabian peninsula.

In the central African region, one of the largest anomalies, the Bangui anomaly, is observed over the center of Africa, at Bangui, (11). The Bangui anomaly characterised by intense negative amplitude, lies along the central Pan-African belts, just north of the Congo craton. The southern flanking positive anomaly, (12), is situated over the thick sedimentary basin of the northern region of Congo basin, (13). The southeast extension of this anomaly is observed over the Kibalian block, (14). The anomaly pattern over the Tanzanian craton, (15), southeast of Congo craton, show a moderate negative. A moderately negative anomaly is observed over the Kasai craton, (16). Further south, a strong positive anomaly is seen over the western region of Angolan craton, (17), while only of moderate intensity over the eastern region. The *initial model* magnetic anomaly map shows a similar trend of the anomalies over the Central Pan-African belt and Congo Basin. However, a large part of the amplitude is yet unaccounted for. This anomaly is studied in detail in chapter (5) where a possible source for the anomaly is investigated. The anomaly pattern over the Tanzanian craton, southeast of Congo craton, is in good agreement with the observations. Most of the Kasai-Angolan craton, located south of the Congo craton, has rock types of low susceptibility and hence a weak negative anomaly is predicted over the region, in agreement with observations. A stretch of positive anomaly observed over the western region of Angolan craton is not reproduced in the *initial model* map. This observed positive anomaly lies over the exposed Archean rocks and the adjoining volcanic rocks in the Kunene region, located in southern region of Angolan craton.

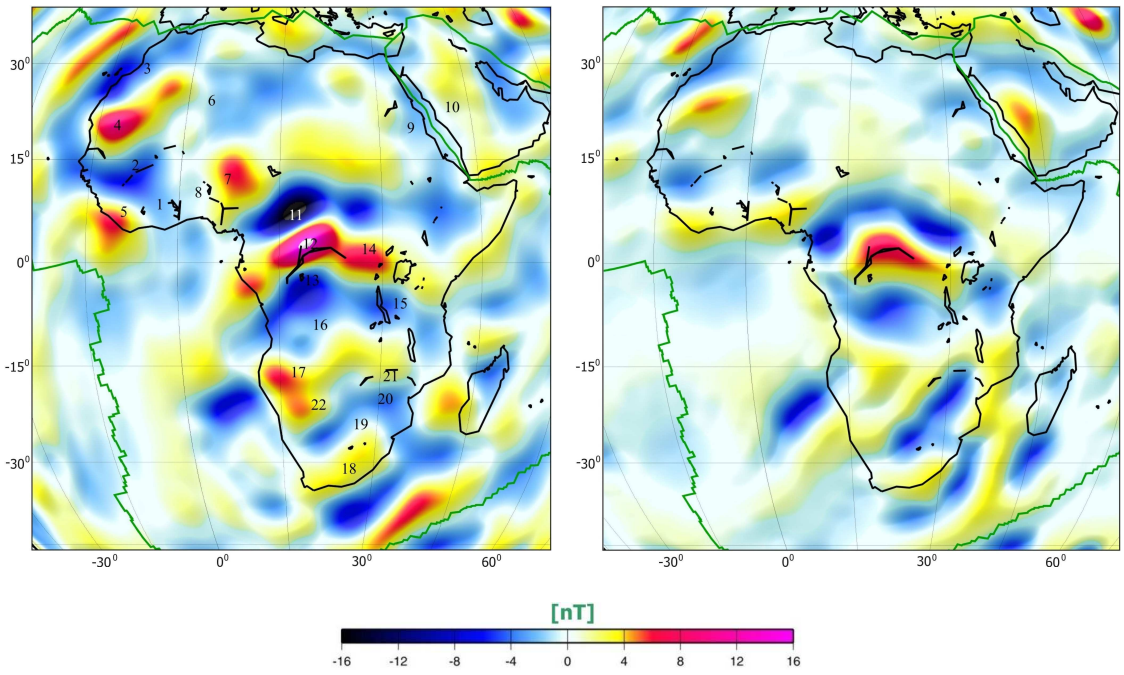

Fig. 4.8a. Observed vertical field anomaly map for spherical harmonic degrees 16-80 at an altitude of 400 km for the African craton.

Fig. 4.8b. *Initial model* vertical field anomaly map for spherical harmonic degrees 16-80 at an altitude of 400 km for the African craton.

In south Africa, the southern portion of the Namaqua-Natal belt, extending up to the Cape fold belt shows a prominent positive, (18), and can be seen both in the observed and predicted map. A long stretch of negative anomaly is observed all along the Kaapvaal craton, (19). This anomaly trend turns eastward where it terminates over the Limpopo mobile belt, (20). The region north of this belt is marked by a weak positive anomaly and it overlies Zimbabawe craton, (21). The region of Damara fold belts, (22), trending NE-SW, located east of Kaapvaal craton, and mostly overlain by the Kalahari sands, appear weakly magnetic over its eastward extension but moderately magnetic over its western region. However, a weak positive anomaly is observed over the western boundary, immediately south of Angolan craton. The predicted vertical field magnetic anomaly map for South Africa is in good agreement with the observations. A positive anomaly over the Namaqua-Natal belt matches well with the observed while the long extended anomaly over the Kaapvaal craton is in good agreement as well. However, this anomaly extends further north over the Zimbabwe craton and the anomaly over the Limpopo belt is only partly reproduced. The anomaly pattern over the Damara fold belts agrees well with the observed, though a part of the positive anomaly in the western region is yet unaccounted for.

4.2.7 Australian craton

This thoroughly studied continent both by ground and airborne geophysical surveys, consists of diverse geological units. Most prominent among them are Pilbara and Yilgarn cratons in the east, with many Proterozoic belts in the center of the continent. Mayhew and Johnson (1987), using Magsat data, provided a magnetisation map using an equivalent source model. Later Mayhew et al. (1991) estimated values for the total vertical integral of magnetisation across the Yilgarn block.

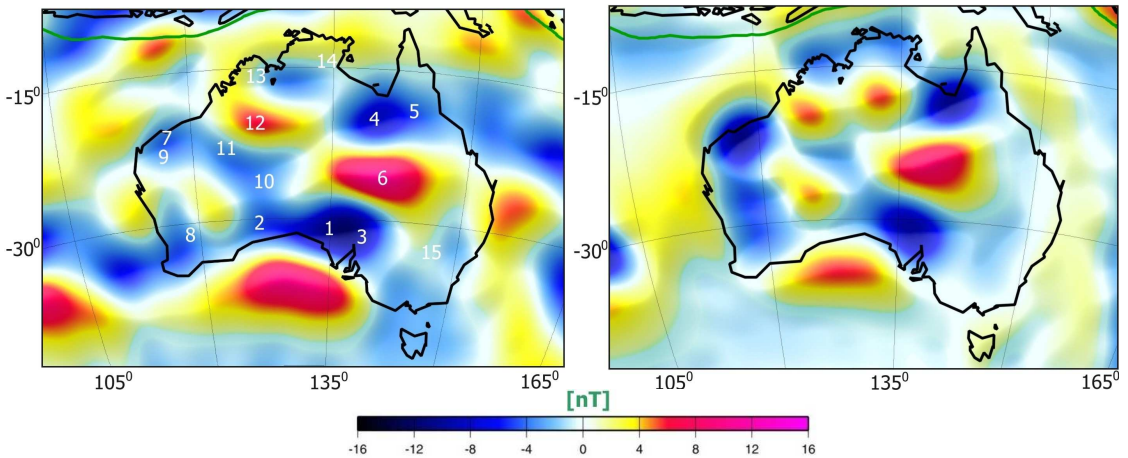

Fig. 4.9a. Observed vertical field anomaly map for spherical harmonic degrees 16-80 at an altitude of 400 km for the Australian craton.

Fig. 4.9b. *Initial model* vertical field anomaly map for spherical harmonic degrees 16-80 at an altitude of 400 km for the Australian craton.

The CHAMP observed vertical field magnetic anomaly map of the Australian continent is shown in Figure (4.9a). A large negative anomaly is observed over the Gawler craton (1), over the western segment of largely buried Nullarbor block, (2), and over the Adeladean

syneclise, (3), located east of the Gawler craton. An intense negative anomaly is observed over the region of Mount Isa Inlier, (4), and Georgetown Inlier, (5), located in the northeast region of the continent. Between Mount Isa Inlier in the north and the Gawler craton in the south lies a high positive anomaly, (6), a region covered by thick Phanerozoic sediments. Interestingly, the negative anomalies over the Archean blocks of Pilbara, (7), in the north and Yilgarn, (8), in the south are of low intensity. A negative anomaly pattern is associated with the banded iron formations of Hamersley basin, (9). An anomaly pattern is also observed extending from the Pibara craton to the central Musgrave ranges, (10), which overlie the sedimentary basin of Paterson province, (11). In central Australia, north of Arunta Ranges, lies an extended positive anomaly, (12). A weak anomaly pattern can be observed in the northern region of the Australian continent, over the Kimberley, (13), and McAurthur, (14), basin. The east Australian region, (15), mostly covered by the Phanerozoic cover appears almost non-magnetic at satellite altitude.

Magnetic anomaly map for the vertical component is computed for the susceptibility distribution (Appendix IX) for various geological units of Australian continent (Fig. 4.9b). The tectonic map for the Australian craton is shown in Figure (2.9). The anomaly observed over Gawler craton, Nullarbor block and over the eastern adjoining Proterozoic belts agrees well with the observed anomaly map. This modelling result confirms the Archean basement below the Adeladean syneclise. Largely buried Nullarbor block is also present west of Gawler craton and the anomaly pattern over it confirms its existence. Though, a part of anomaly over the Nullarbor block is not predicted well over the region. The region over the Mount Isa Inlier and Georgetown Inlier shows an anomaly of low intensity that is in agreement with the observations. A large positive anomaly located over the region between Mount Isa in the north and Gawler craton in the south is reproduced well. The positive anomaly north of Arunta range is only partially predicted in the *initial model* map. Anomalies computed over the Pilbara craton and Yilgarn craton agree well though the predicted anomaly over the Pilbara craton is more intense. A very strong negative anomaly is also observed over the Hamersley Basin whose amplitude is in surplus when compared with the observations. The anomaly observed over the Paterson province, however, is not reproduced in the predicted map. Anomaly computed over Kimberley and McArthur basin agrees only partially with the observations. In east Australia, the anomaly patterns between the observed and computed map is in good agreement.

4.2.8 Greenland

This country, which is covered by 90% with ice, has rarely been investigated in detail using magnetic satellite data. The geological information for Greenland has only been inferred on the basis of exposure of rock types at the periphery. However, in its central region, geological units have always been a mystery. Lately, more seismic results have thrown some light onto possible tectonic units of Greenland (Dahl-Jensen et.al, 2003) in its interior. Langel and Thorning (1982) used POGO satellite data to estimate a magnetisation map for Greenland, but no effort was made to interpret the anomalies.

The vertical field anomaly map of Greenland is shown in Figure (4.10a). A high positive anomaly is observed over the Archean block of southern Greenland, (1). Over the northern region of Greenland there is an anomaly, (2), that extends from East to West. The central Greenland, (3), show negative anomaly pattern of moderate intensity.

The vertical component map is computed using the susceptibility distribution of rock types exposed at the periphery of the country (Appendix X). The tectonic map of Greenland is shown in Figure (2.4). The predicted anomaly over the southern Archean block shows a good agreement with observations (Fig. 4.10b). The anomaly pattern over the northern region shows a broad anomaly that extends from northern Greenland to the central region of the country. The predicted anomaly, though it partly agrees with the observed anomaly, is significantly more extended in south direction. This extension of predicted anomaly in southward direction is caused by the crustal thickness variation within Greenland. The extent of this anomaly is investigated further in chapter 5.

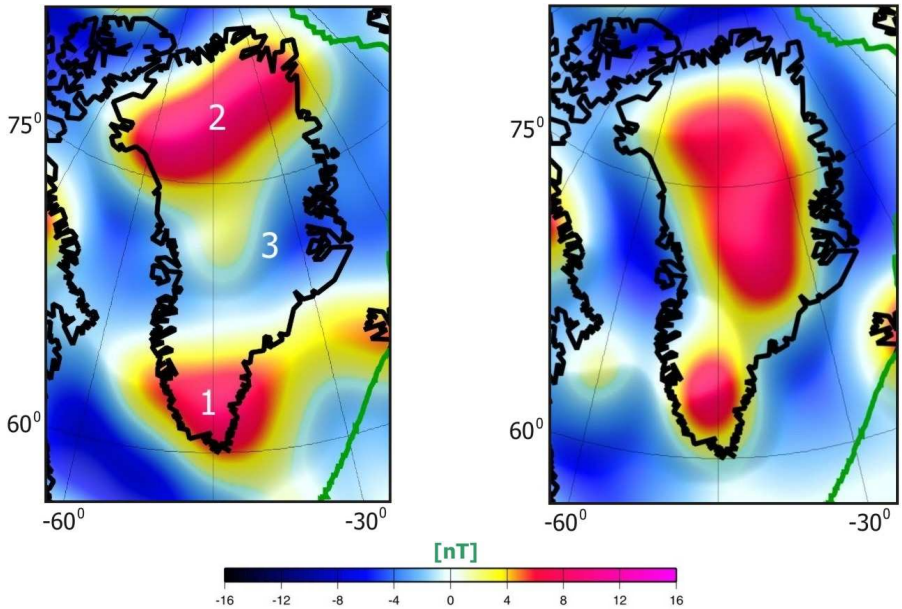

Fig. 4.10a. Observed vertical field anomaly map for spherical harmonic degrees 16-80 at an altitude of 400 km for the Greenland.

Fig. 4.10b. *Initial model* vertical field anomaly map for spherical harmonic degrees 16-80 at an altitude of 400 km for the Greenland.

4.2.9 Antarctic craton

Not much is known about this continent as far as regions covered with ice are concerned. Though intense exploration work is carried out in Antarctica, it is mostly restricted to the exposed geological regions. Using satellite data, efforts were made to estimate a crustal field model over the south pole (Langel and Thorning, 1982; Ritzwoller and Bentley; 1982; Alsdorf et al., 1994; von Frese et al., 1997). von Frese et al. (1997, 1999) made an effort to model these anomalies based on satellite gravity and magnetic data. Recently, Kim et al. (2002) mapped the regional anomalies over Antarctica using Ørsted satellite data.

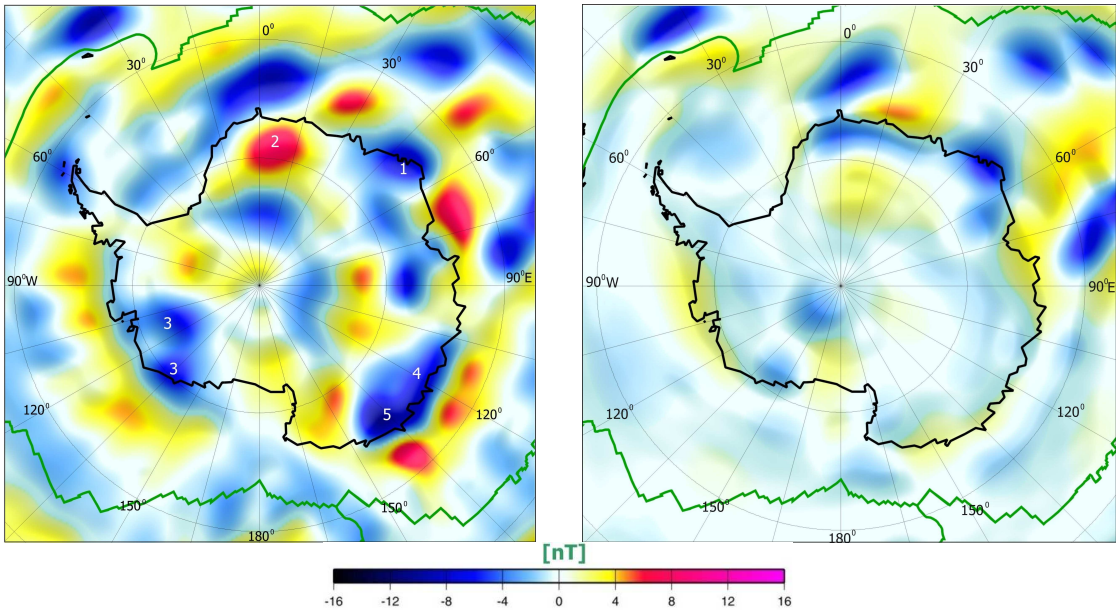

Fig. 4.11a. Observed vertical field anomaly map for spherical harmonic degrees 16-80 at an altitude of 400 km for the Antarctica.

Fig. 4.11b. *Initial model* vertical field anomaly map for spherical harmonic degrees 16-80 at an altitude of 400 km for the Antarctica.

The observed vertical field anomaly map over the continent of Antarctica is shown in Figure (4.11a). The map shows some of anomalies, not only over the geological regions exposed, but also over the regions covered with ice. The most prominent regions that are exposed and an anomaly associated with it are Napier and Rayner Complex, (1), located south of Kerguelen plateau and lying between longitude 45^0-60^0 East. An elongated large positive anomaly is observed over the Dronning Maud Land, (2). There are two other anomalies located over the region between 90^0-150^0 West, (3), centered on 80^0 South. The other anomalies that lie along the coast of Antarctica is located over Wilkes Land, between 105^0 E and 145^0 E, (4), and one centered on 135^0 W, (5). There are some anomalies in the interior of the continent, but they are over the ice-covered region and their geological association cannot be ascertained at this moment.

Precambrian units of the exposed Antarctica regions are modeled and their susceptibility distributions are shown in Appendix XI. The tectonic map for the Antarctica craton is shown in Figure (2.10). The predicted anomaly pattern over Rayner and Napier complex is reproduced well (Fig. 4.11b). An anomaly of low intensity observed east of it is, however, not reproduced. The anomaly over Dronning Maud Land is not reproduced in the *initial model* anomaly map. A significant portion of anomaly over the region lying between 90^0-150^0 is not produced. An anomaly observed over the region centered on 135^0 W, between 105^0-145^0 E, is completely missing from the *initial model* map. The anomaly observed at other regions is not at all reproduced in the predicted map due to the lack of geological information for these ice covered regions.

4.2.10 Oceanic crust

The oceanic crust is of uniform thickness across the globe. The oceanic plateaus occupy 10% of the oceanic region. Remanent magnetisation dominates in the oceanic crust, as evidenced from the seafloor spreading anomalies. Harrison (1987) and Tivey (1996) reproduced these spreading anomalies by assuming the magnetisation restricted to layer 2. However, at the satellite altitude these spreading anomalies cancel each other. It was argued by Arkani-Hamed and Strangway (1986c) that upper mantle also contributes to the long wavelength anomalies observed over the oceans. Based on the model study of subduction zones at Kuril-Kamchatka trench, they reported the upper 35 km of oceanic upper mantle to be magnetic with an effective magnetic susceptibility of 0.0085 SI. Thus possible contribution of magnetisation from the upper mantle is not ruled out (Arkani-Hamed, 1988, 1991). However, Thomas (1987) proposed a model in which viscous and induced magnetisations were the main sources of the long-wavelength anomalies seen in satellite data.

The observed vertical field magnetic anomaly map of the world is shown in Figure (4.12). This section deals with the study of anomalies observed over the oceanic region. Anomalies of moderate intensity (2 – 4 nT) are seen over all of the major oceans of the world. The magnetic strips of highs and lows parallel to the mid-oceanic ridges, so prominent in the aeromagnetic surveys, are mostly absent at satellite altitude, except for few lineations parallel to the mid-oceanic ridges observed over the North Atlantic Ocean. This is due to the fact that fields from the alternating remanent magnetisations of the oceanic floor spreading magnetic anomalies are nearly cancelled at satellite altitude. However, Hayling and Harrison (1986), Purucker et al. (1998) modeled anomalies associated with KQZ (Cretaceous Quiet zones) in the Atlantic Ocean. The oceanic crust in these zones, being wide enough to retain magnetic signature of the Cretaceous normal, result in measurable anomalous fields at satellite altitude (LaBrecque and Raymond, 1985). There are anomaly patterns over the oceanic region that do not seem to have a geological source, and could be uncorrected external signals and high degree main field. It is due to the fact that the anomalies over the oceans are generally much weaker that the main field of degrees 16-20 can be seen there. Even then, the comparison of the observed map with the world geological map makes it clear that most of the observed anomalies over the oceanic regions are due to the scattered oceanic rises, mounts and plateaus, where the oceanic crust is generally thicker than the surrounding crust. Some of these plateau-like structures are dismembered part of continents, especially in the Indian Ocean, created as a result of Gondwana breakup.

The modelling of oceanic crust is done using the 3-layered model for oceanic crust of which the top layer of sediments is considered non-magnetic. The susceptibility distribution used for modelling is shown in Appendix XII. The *initial model* magnetic anomaly map for the vertical component over the oceanic region is shown in Figure (4.13). The predicted anomaly over the oceanic crust does not show interesting anomaly patterns, unlike those in observations where weak anomaly patterns are scattered everywhere. Over the oceanic plateaus and rises, the anomaly patterns in the *initial model* map agree well with the corresponding region of the observed map. Since the remanant

magnetisation of magnetic strips of alternate polarity across the mid-oceanic ridges is not included in the model, there are no magnetic signatures in the *initial model* map related to these alternate highs and lows. Considering a uniform layering of the oceanic crust, the predicted anomaly pattern is in good agreement with the observed magnetic anomaly map.

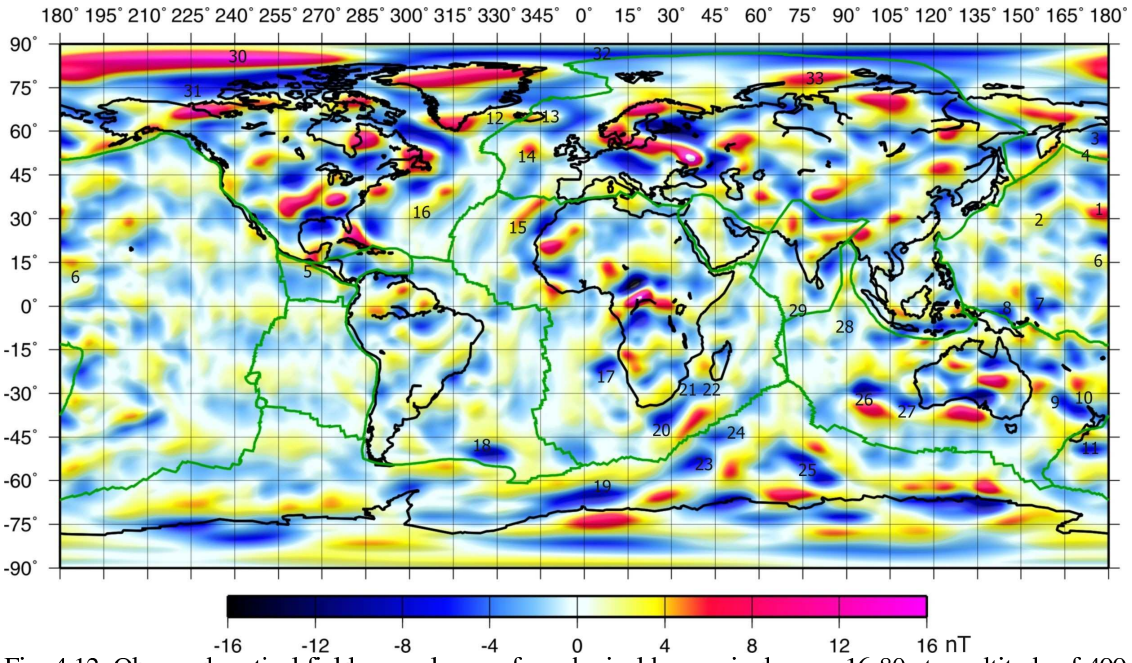

Fig. 4.12. Observed vertical field anomaly map for spherical harmonic degrees 16-80 at an altitude of 400 km shown in cylindrical equidistant projection. The numbers shown in white is marked over the plateaus.

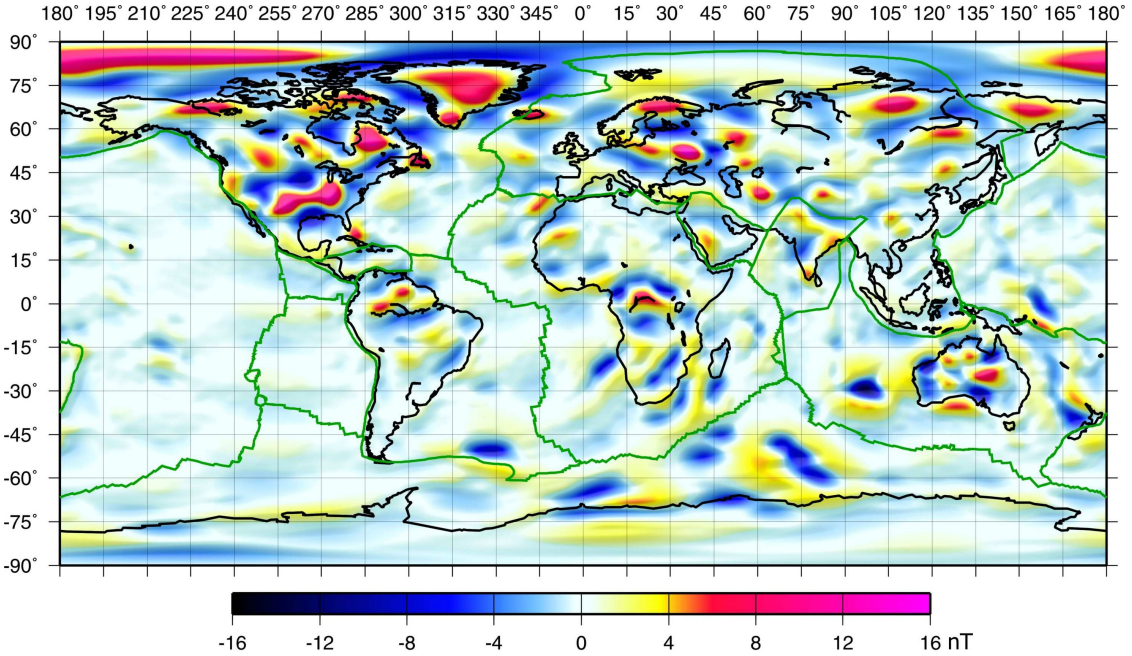

Fig. 4.13. Predicted vertical field anomaly map (*initial model*) for spherical harmonic degrees 16-80 at an altitude of 400 km shown in cylindrical equidistant projection.

The following section compares the observed and predicted anomalies associated with the oceanic plateaus, rise and scattered microcontinents for each of the Oceans.

4.2.11 Oceanic plateaus

Apart from interpretation of anomalies over the oceanic crust, the anomalous pattern observed over the plateaus and rises have generated sufficient interest to model these anomalies. One of the most comprehensive studies was conducted by Johnson (1985), who attributed the dipole anomaly over the Broken Ridge, to be due to significantly induced magnetisation and partly remanent. Bradley and Frey (1988) modeled the Kerguelen plateau and Broken ridge similarly. Fullerton et al. (1994) studied all the anomalies over the southwestern Indian Ocean region. Toft and Arkani-Hamed (1992) examined volcanic plateaus and the effects of the KQZ in the Pacific Ocean. Significant studies were conducted by Alsdorf (1991) over the south Atlantic Ocean and by Hayling and Harrison (1986) over the north and central Atlantic Ocean, while, Taylor (1991) studied the eastern Indian Ocean. All the above studies used Magsat satellite data for modelling and interpretation. Using CHAMP satellite data, we conducted similar studies and the following paragraphs describe the modelling results.

The observed anomalies over the Pacific Ocean as shown in Figure (4.12) are largely of moderate intensity. A prominent positive anomaly lies over the Hess rise, (1), northwest of the Hawaiian Islands, and a very low amplitude positive anomaly is observed along the Shatsky rise, (2). North of Hess Rise, in the Bering Sea, (3), lies a positive anomaly of moderate intensity, all along the Aleution arc, (4), that is attributed to the subduction zone of the northern Pacific region (Clark et al., 1985). A strong positive anomaly is observed at the southwest coast of Mexico, (5), also attributed to the presence of subduction zones in the region (Counil and Achache, 1987). Hawaiian ridge, (6), does not show up in the satellite altitude magnetic anomaly map, but weak anomaly patterns are observed in its surrounding. One of the largest negative anomalies, observed across the equator is associated with Ontong-Java plateau, (7), and another along the equator is observed west of it, (8), over the oceanic crust. Further south, due northwest of New Zealand, lies an intense negative anomaly associated with the Lord Howe Rise, (9). The anomaly extends not exactly along the rise, but in between the Lord Howe rise and Norfolk plateau, (10), in the northwest direction and abruptly terminates at the center of the Lord Howe rise. It then reappears as an oval-shaped anomaly over the northern tip of the rise. Another intense negative anomaly is observed over the center of Cambell plateau, (11), south of New Zealand.

Based on the VIS model of oceanic plateaus and rises (Appendix XII) the vertical field magnetic anomaly map is computed and is shown in Figure (4.13). A good correspondence can be seen between the predicted and observed anomaly patterns over the Ontong-Java plateau. Over the Shatsky rise in the north, a strong positive is noticed at the center of long stretch of rise, however, over the Hess rise, a large part of anomaly is yet unaccounted for. In the southern hemisphere, northwest of New Zealand, the predicted anomaly pattern does not follow the observations and appears shifted south over the Lord Howe rise and not in between the rise and Norfolk plateau which features

so prominently in the observed map. A negative anomaly is seen at the northern edge of the Lord Howe rise in agreement with observations. The negative anomaly south of New Zealand is also not predicted in the *initial model* map. In short, the anomalies corresponding to all of the plateaus in the Pacific oceanic region are only partly recovered and require further investigation.

Both the North and South Atlantic Ocean is marked by the presence of scattered magnetic anomalies corresponding to oceanic plateaus (Fig. 4.12). In the north, from the southern base of Greenland to the western coast of Iceland, (12), a positive anomaly of moderate intensity is observed that extends beyond the eastern coast of Iceland until the Faeroe-Rockall plateau, (13). Over the Faeroe-Rockall plateau lies an intense negative anomaly and over its southern edge, (14), a strong positive anomaly is observed, not exactly overlying any oceanic plateau region. Further south, along the northwestern banks, (15), of West African craton, an extended positive anomaly is observed that corresponds to Madeira and East Canary plateaus. However, the shorter extent of these plateaus falls short of explaining the much larger extent of the anomaly. An anomaly of similar pattern and of the same length is observed on the western side, (16), of the north Atlantic mid-oceanic ridge axis without actually corresponding to any plateau region. Purucker et al. (1998) attributed these patterns to the Cretaceous Quiet Zones (KQZ). In the south Atlantic, two major anomalies mark their presence, one is over the Walvis ridge, (17), off the western coast of Central-South Africa and the other is over the eastern edge of North Scotia ridge, (18), off the coast of Falkland Islands, South America. Further south, flanking the 0 degree meridian, off the coast of Antarctica, lies a large elongated anomaly that partly overlies the Maud rise, (19), and the rest of it extends beyond the present known subsurface geological boundary of Maud rise.

Following a similar methodology as for the Pacific region, the oceanic plateaus in the Atlantic Ocean are modelled and a vertical field magnetic anomaly map is computed (Fig 4.12). The predicted anomaly between the southeastern region of Greenland and the eastern coast of Iceland does not agree with observations. An intense positive anomaly is predicted over Iceland, not in agreement with observations. The surplus anomaly observed over the Iceland needs further investigation. Further south, over the southern edge of Rockall plateau an anomaly is seen in the *initial model* map but the anomaly appears shifted further south. Positive anomaly corresponding to Madeira and East Canary Islands, off the coast of West African craton, agrees well with the observed map although a part of the southern half of the anomaly is not reproduced. Anomalies corresponding to magnetic highs and lows observed parallel to the North Atlantic mid-oceanic ridges are not reproduced due to the absence of oceanic plateaus in these regions. Hence, they were not modelled. In the south Atlantic Ocean, the anomaly off the coast of mid-south African continent, over the Walvis ridge, is reproduced well, although a part of the amplitude is yet unaccounted for. The same situation holds for the anomaly pattern over the eastern edge of North Scotia ridge, South America. An anomaly over the Maud Rise is also not reproduced in the *initial model* anomaly map.

The Indian ocean (Fig. 4.12) is littered with anomalies of all shapes, mainly overlying the oceanic plateaus and dismembered bodies created as a result of Gondwana breakup.

Prominent negative anomaly is observed over the Agulhas plateau, (20), at the southern coast of Africa, which extends further north along the Mozambique ridge, (21), and continues over the Madagascar plateau, (22). Further south, two small oval-shaped anomalies are seen over the Conrad rise, (23), and Crozet plateau, (24). Southeast of these plateaus lies the great elongated Kerguelen-Gaussberg ridge, (25), which is also associated with a strong negative anomaly. Sharing the same origin as the Kerguelen ridge is the Broken ridge, (26), that now lie on the northern side of the mid-oceanic ridge, off the western coast of Australia. An intense negative anomaly can be observed over it. The anomaly pattern, however, follow the series of plateaus that extend up to the Naturliste plateau, (27), just at the coast of southwest Australia. There is no anomaly observed at satellite altitude corresponding to the 90 East ridge, (28), and the Laccadive ridges, (29), off the south of Indian peninsula.

The *initial model* vertical field anomaly map for the Indian Ocean is shown in Figure (4.13) and the susceptibility distribution is shown in Appendix XII. A large number of significant anomaly patterns are reproduced. The anomaly over the Agulhas and the Mozambique plateau is reproduced well but a strong negative anomaly is observed over the Madagascar rise, moderately higher in amplitude than the observations for the same region. Also noticeable is the anomaly extent, continuing unterminated from the Mozambique plateau to the Madagascar rise in the observed map. This is absent in the predicted map. The anomaly over the Conrad rise and Crozet plateau agrees with the observations and so does the anomaly over the elongated Kerguelen plateau. However, a part of the predicted anomaly over the northern portion of Kerguelen plateau does not agree with observations. The large anomaly over the Broken ridge agrees well with the observed map but much of the positive anomaly south of it is not produced. Furthermore, the meandering anomaly pattern, off the southwest coast of Australia, is not reproduced, nor can an anomaly be seen over the Naturliste plateau.

The Arctic Ocean (Fig. 4.12) is marked by the presence of a very large and strong positive anomaly associated with the Alpha ridge, (30), just north of Greenland. The Alpha ridge (Jackson and Johnson, 1986; Weber, 1986) is generally considered to be of oceanic origin (Forsyth et al., 1986a, 1986b). However, the work of King et al. (1964) and Taylor (1983) suggests it to be a continental fragment and the dispute is yet unresolved. The anomaly located north of Canada, (31), is an intense negative anomaly and corresponds to Canada Basin. The region of Kara Sea, (32), is largely non-magnetic. However, an anomaly, (33), is observed north of Taimyr fold belts, between Novaya Zemlya and Severnaya Zemlya Islands. The anomaly could be due to the submerged Kara massif, which is composed of crystalline Precambrian rocks covered by Paleozoic sediments (Khain, 1985).

The plateaus in the Arctic region are modelled and the corresponding computed vertical field magnetic anomaly map is shown in Figure (4.13). The predicted anomaly map agrees well with the observed map as a whole. The intense positive anomaly over the Alpha ridge is reproduced very well; even the shape of the anomaly is in almost total agreement except for a small bulge at the southern edge of the anomaly. The anomaly over the Canada Basin also matches well with the observed map. The anomaly pattern

over the Kara Sea appears largely non-magnetic in agreement with the observations. A strong high observed over the northern coast of Taimyr fold belt is, however, absent from the predicted map. Hence, further investigations are required in order to identify the source of the anomaly.

I have described the modelling results for the major magnetic anomalies patterns observed over the diverse geology of the continental region, over the more uniform oceanic crust and over the poorly known oceanic plateaus. Definitely, some predicted anomaly patterns agree with the observed anomaly map while at other regions there is disagreement with the observations. Based on these results, our efforts would now be to find the sources for the anomalies that are in disagreement with the observed anomaly map. Over the continents, only 29% of Precambrian rocks are exposed, while the rest of the regions are buried by younger Phanerozoic cover. Thus, using the present flexible modelling procedure that allows us to modify the boundary of a geological unit, our efforts are to trace the possible extension of Precambrian units underlying the young cover and to provide answers to some of the key issues of global crustal field modelling. The following chapter will concentrate on some of such selected regions that have not been explained by our *initial model* but require further investigation to find the sources for the missing anomalies of the predicted map. Over the oceanic region, the presently known subsurface geology and its composition especially for some plateaus, is inadequate to explain some of the anomaly patterns. This would need further investigation to sort out the problems over the oceanic region. However, the present work does not pursue further the anomaly patterns over the oceanic regions but concentrates on modelling the anomalies over the continental region.